A Method for Studying the Influence of the Underlying Surface on the Control Algorithms for Low-Flying Aircraft

Vuong Anh Trung

Faculty of Aviation Technology, Air Defence-Air Force Academy, Ha Noi, Vietnam
Email: vuonganhtrung@gmail.com

***Abstract*—When an aircraft flies at a high altitude, it is not influenced by the terrain surface below on its parameters and sighting (underlying) surface conditions. However, when flying at low altitude, the conditions of the terrain below significantly affect the aerodynamic parameters of the aircraft. The parameters related to the flying environment include temperature, pressure, and wind status. When the parameters change, it will affect the aircraft control algorithm. The paper considers a methodology for studying the underlying surface's influence on low-flying aircraft control algorithms. The method allows the study of the influence of the underlying surface on control algorithms for low-flying aircraft based on defining Digital Terrain Maps (DTM) and Maps of Real Components (MRC) libraries available. Simultaneously, an example of the algorithm was carried out to estimate the methodical error of the baro-inertial channel due to a change in the isobar along the flight path.**

***Keywords*—low-flying aircraft, digital terrain maps, maps of real components, digital complex mathematical, baro-inertial**

I. Introduction

Low-flying aircraft features, especially the accuracy of flight control algorithms, are significantly affected by environmental parameters and screening (underlying) surface conditions. The parameters related to the flying environment include temperature, pressure, and wind status. The underlying surface is a set of reliefs along the flight trajectory with ground terrain [1–3]. Air environmental changes can change within known-possibility limitations. However, the underlying surface features along the flight path usually vary and are difficult to describe analytically.

There is no doubt that the information about ground objects that are presented on geographical maps has an unregulated low accuracy. Furthermore, the composition and characteristics of the ground objects may change after the creation of the initial cartographic material [4, 5]. Consequently, studying the underlying surface's influence on low-flying aircraft control algorithms is crucial in control theory. The variety of the underlying surface terrain changes the environment status, leading to a large variability in flight conditions. Carrying out full-scale tests in such a variety of conditions is extremely difficult. Nelson [6] and Fotuhi *et al*. [7] mentioned the lower surface's influence on the aircraft's aerodynamic parameters but only stopped at the modeling issue. Xu *et al.* [8] and Fotuhi *et al.* [7] developed a lightweight and conformable system on the wing surface of aircraft for stall sensing but only addresses the problem of general turbulence control and does not address problems due to the underlying surface. This problem can be solved by mathematical modeling using modern computing facilities. The techniques used in such studies are discussed in this article.

The technique was applied to study the algorithm's accuracy for estimating the baro-inertial channel's methodological error due to a change in the isobar along the flight path. It is intended for use in low-flying aircraft control algorithms to provide accurate vertical channel navigation. A bar and radio altimeter are installed on board as measuring instruments. The parameters of the air environment influence the measurement accuracy of the bar altimeter. The specificity of the radio altimeter is its broad beam, and therefore, its accuracy is influenced by the characteristics of the underlying surface [9–11].

In the algorithm for estimating the methodological error of the baro-inertial channel, the difference between the measured heights (the difference between the baro-inertial and radio heights) and the reference (onboard information about the underlying surface) profiles are passed through two successive nonlinear filters namely thresholds and smoothing filters. The task of the threshold filter is to filter out areas with increased steepness of the relief and containing object compositions. In the threshold filter, the current estimating value is compared with the previously available estimate, and the one that is a priori more accurate is selected from them.

When comparing the estimates, the local steepness of the underlying relief and the sign and magnitude of the change in the filter's input signal are considered. The local steepness of the underlying relief leads to the appearance of an error due to the uncertainty of the location in the horizontal plane. A change in the input signal exceeding

Manuscript received December 1, 2023; revised February 28, 2024; accepted April 28, 2024; published November 18, 2024.

doi: 10.18178/ijmerr.13.6.573-577

the permissible value is obtained due to the analysis of the nature of the relief. In addition, a possible change in the magnitude of the methodical error of the radio altimeter and a possible change in the isobar prepare for the appearance or disappearance of ground objects in the field of view of the altimeter. The task of the smoothing filter is to process the information remaining after rejection. Thus, the performance of this algorithm is significantly influenced by the underlying surface features along the flight path. Further consideration of the methodology will be carried out to illustrate the accuracy of this algorithm.

The proposed methodology consists of the following stages: selection of the underlying surface, determination of the characteristics of the selected relief, selection of intervals and steps of enumeration of the initial coordinate of the flight orthodromy, simulation of the flight of the aircraft, and processing of the simulation results. These are issues that have not been addressed by many studies or have only been limited to general theoretical research to build models [12].

II. Theory and Working Principle of Low-Flying Aircraft

The effectiveness of low-altitude flight and the level of flight complexity depend on the nature of the flight trajectory. Currently, there are two basic types of low-altitude flight orbits.

- Flying over terrain (over obstacles)—Ensures the aircraft maneuvers in a vertical plane.
- Fly to avoid terrain (obstacle avoidance)—Ensure the aircraft maneuvers in the horizontal plane.

In reality, we can combine both types of orbits above. Automating aircraft control in the horizontal plane usually involves automatically stabilizing the aircraft according to a pre-set flight program or the pilot selecting and maintaining maneuvers along a predetermined horizontal plane flight path. The pilot controlling the aircraft maneuvering in the vertical plane in low-altitude flight is much more stressful and complicated because it requires the pilot to make control actions continuously. Controlling a maneuverable aircraft according to a pre-calculated program in the vertical plane is completely possible but requires the aircraft to follow the given trajectory accurately. Therefore, automating low-altitude flight control must ensure continuous measurement of terrain features, and the automatic control system creates flight trajectories directly on the aircraft according to those features. The ideal low-altitude flight trajectory is equidistant from the terrain, meaning it flies over the terrain at a certain altitude. However, in reality, the aircraft does not fly this trajectory because of vertical overload, and the allowable orbital flight angle is limited.

The low-altitude flight control system is a system that ensures the aircraft automatically flies at low altitudes over the terrain and around the terrain by calculating aircraft control parameters along the vertical channel and horizontal channel in case of necessity. The system also ensures flight from dangerous heights. The low-altitude flight system uses forward terrain information mainly using terrain observation radar.

Signals about the observed terrain are fed into the low-altitude flight control circuits. Usually, two methods are applied to control low-flying aircraft:

- The first method is using an automatic stabilization system for terrain slope distance. The essence of this method is to stabilize the distance from the aircraft to the surface (the point considered is in front of the aircraft) on the terrain the aircraft will fly over.
- The second method is applying an automatic control system for flying over terrain. This control system is called an angular system since to control the aircraft over obstacles, the system needs to use the angular position of the predicted point on the terrain relative to the aircraft.

The disadvantage of the above two methods is that the information about the terrain is small, making it challenging to create an optimal flight trajectory to overcome obstacles. The author uses the "hypothetical terrain" method to overcome the above disadvantages. Its essence is to replace real terrain with hypothetical terrain calculated in the computer according to the characteristics and shape of the real terrain that will be flown over. Usually, the terrain is assumed to be flatter, so when creating control commands, the allowable limit values of the orbital angle and vertical overload of the aircraft are considered. After replacing with "simulated terrain", the system performs normal control according to obstacle-overcoming systems. The only difference is that the forecast point is chosen on a predetermined "hypothetical terrain". The "assumed terrain" method allows for a flatter low-altitude flight trajectory closer to the optimal trajectory.

III. Selection of the Underlying Surface

The first stage of the study is the selection of the underlying surface for modeling. For this, several libraries of Digital Terrain Maps (DTM) and Maps of Real Components (MRC) exist. The DTM library (digital terrain models are recorded data in a specific format and codes) includes a set of typical DTM and a DTM passport. The DTM passport contains the parameters included in the DTM library: card number, discrete with horizontal coordinates (*dx, dz*), map size, and coordinates of the starting point of the map.

The MRC library also includes a set of typical MRC and an MRC passport that contains typical MRC model forests, various settlements, and other single and group objects. The main characteristics of MRC are the height and density of ground objects—object height changes in a given interval according to a certain distribution law. Filling density is the ratio of the area filled with the object composition to the total area of the map. The structure of the MRC passport is similar to that of the DTM passport.

To set the relief of the underlying surface along the flight path, the DTM must be selected, and the coordinates of the beginning and the length of the orthodrome are pre-set. If it is needed to model the object composition, select SM, superimposed on top of the selected relief along the flight orthodrome [13–15].

IV. Definition of DTM Characteristics

In the second stage, determining the selected relief's characteristics is necessary. DTM is characterized by the height (H) and the steepness (α) of the relief, where:

$$\begin{cases} \alpha_x = arctg(\frac{H_i - H_{i-1}}{dx}) \\ \alpha_z = arctg(\frac{H_i - H_{i-1}}{dz}) \\ \alpha = \max(\alpha_x, \alpha_z) \end{cases} \quad (1)$$

here: i=1÷n; d_x, d_z, The discrete horizontal DTM. To determine these characteristics, we construct the histograms of the distribution of heights and relief steepness according to DTM. Let us choose three typical DTMs from the library to conduct research. A special program has been created to construct histograms of the distribution of the characteristics of the reliefs. In Fig. 1, for example, the histograms for DTM 1 are shown. Based on the histograms, we determine the mathematical expectations and standard deviations of the constructed characteristics (Table I). The obtained numerical characteristics make it possible to compare the DTM regarding the degree of ruggedness.

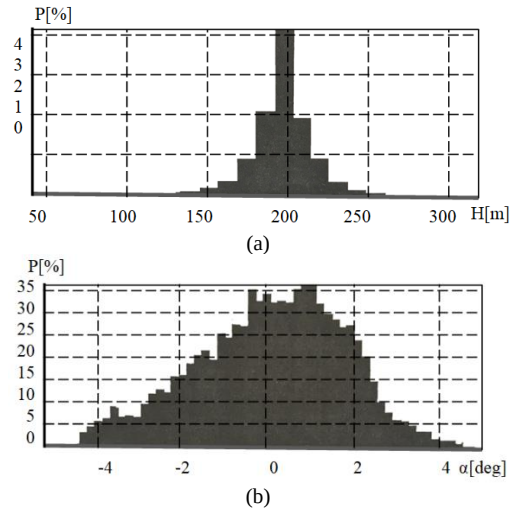

Fig. 1. Histograms of relief characteristics, (a) relief heights, (b) relief steepness.

TABLE I. Characteristics DTM

Number DTM	M_H [m]	σ_H [m]	M_α [deg]	σ_α [deg]
1	174	48	0.03	1
2	372	62	–0.03	2.14
3	272	239	0.24	4.27

V. Choice of Intervals and Steps of Enumeration of the Initial Coordinate of the Flight Orthodromy

Next, the intervals [X_{H1}…, X_{H2}], [Z_{H1}.., Z_{H2}] and the steps of enumeration ΔX_H, ΔZ_H of the initial coordinate of the flight orthodrome in the DTM area are selected, and then the required number of orthodromies. The resulting arrangement of orthodoxies is shown in Fig. 2. As a result, the number of orthodoxies is equal to:

$$N_{orth} = (\frac{X_{H_2} - X_{H_1}}{\Delta X_H} + 1) \times (\frac{Z_{H_2} - Z_{H_1}}{\Delta Z_H} + 1)$$

In the study of the algorithm [16–18] under consideration, the steps of enumerating the initial point of the orthodromy ΔX_H = 10km and ΔZ_H = 1.2 km were selected. Orthodrome length L = 50 km. Thus, 336 orthodromies for DTM 1, 315 for DTM 2, and 328 for DTM 3 were obtained.

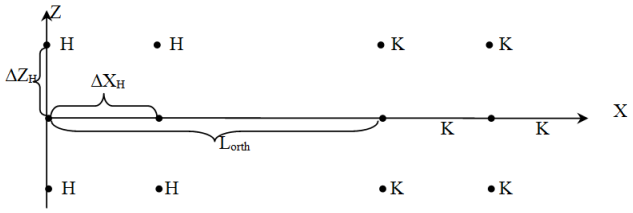

Fig. 2. Location of orthodromies on DTM. The beginning of orthodromy; K- the end of orthodromy.

VI. Simulation of the Flight of An Aircraft

Let us consider the initial conditions for modeling. For the considered algorithm, the following initial simulation errors are specified [16, 17]:

- Methodical error of the arterial channel, linearly increasing with an inclination of 120 m per 100 km;
- The error of the navigation system in the horizontal plane is 100 m.

To work out control algorithms for aircraft, a Digital Complex Mathematics (DCM) was created, which, according to the assigned flight task, simulates the movement of the aircraft and works out the control algorithms. The structure of the DCM is shown in Fig. 3. The DCM was used to simulate the flight of an aircraft under the conditions selected above. For this, the control program sets the simulation conditions: DTM number; X_{H1}, X_{H2}, Z_{H1}, Z_{H2}, ΔX_H, ΔZ_H, MRC number; and the rest of the simulation conditions.

The control program contains all the selected flight orthodoxies. For each orthodromy, a flight position is set, and the flight trajectory is simulated utilizing a simulation program which includes the object models and control algorithms and where the necessary output parameters of the control algorithms (output information) are selected, obtained during the simulation of each flight task [18].

The error and the a priori estimate of the algorithm error should be received as the output parameters of the considered algorithm [19–21]. In this case, the error determines the algorithm's accuracy, and the a priori estimate is the expected error module. As a result of the simulation with the DCM, a set of output information was obtained for each of the selected DTM.

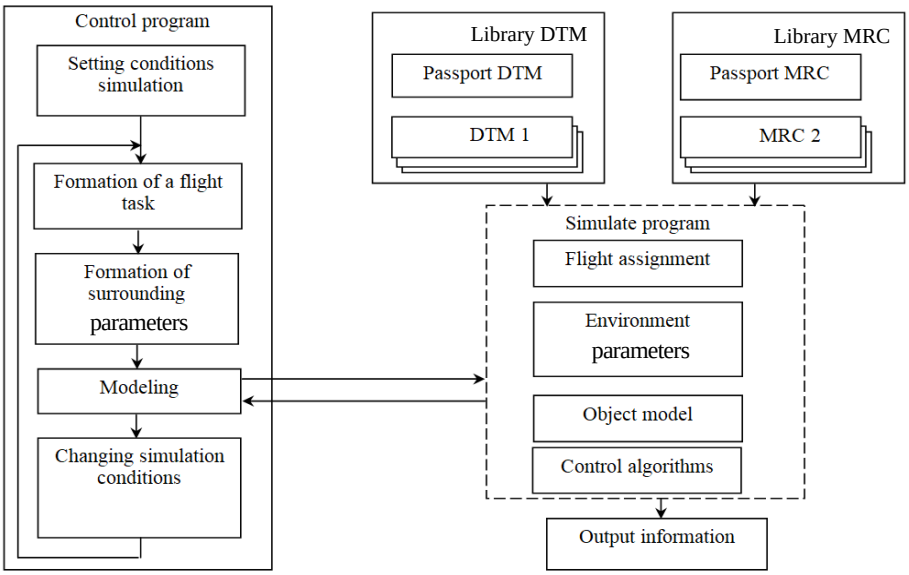

Fig. 3. Structure of DCM.

VI. Results and Discussions

The resulting set of output information will be processed statistically. For this, a program in Matlab for constructing histograms of output parameters has been created (Fig. 4 shows the modeling results on DTM 1). Using the constructed histograms, we determine the output parameters' mathematical expectations, standard deviations, and maximum values (Table II).

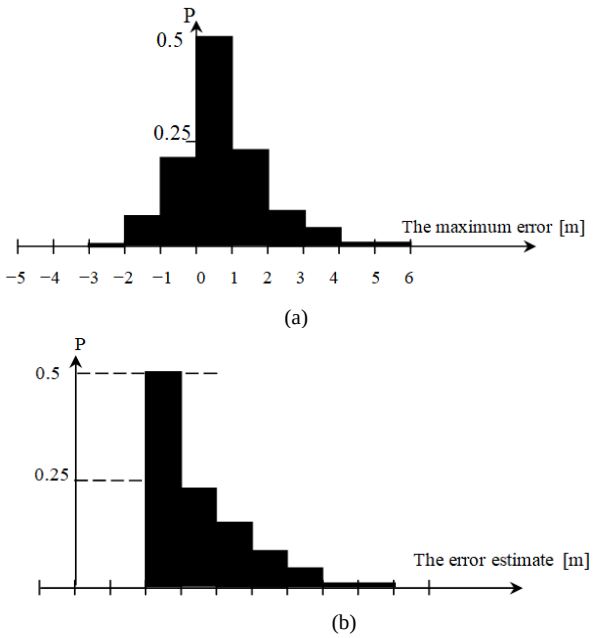

Fig. 4. Histograms of output parameters, (a) error, (b) error estimates.

TABLE II. Output Parameters

Number DTM	Error			Error Estimates		
	M [m]	σ [m]	Max [m]	M [m]	σ [m]	Max [m]
1	0.7	1	5.3	1.7	0.7	4.7
2	0.7	2.3	9.2	4.2	1.7	10.8
3	1.1	3.4	15.6	5.4	3.4	22.3

Now, the obtained simulation results can be compared with the characteristics of the selected DTM to get analytical dependencies. Let us construct, for example, a graph of the dependence of the maximum error and the error estimate on the standard deviation of the steepness of the relief (Fig. 5). From the obtained dependence, it can be concluded that the maximum error and the error estimate increase in proportion to the steepness of the relief [22–24].

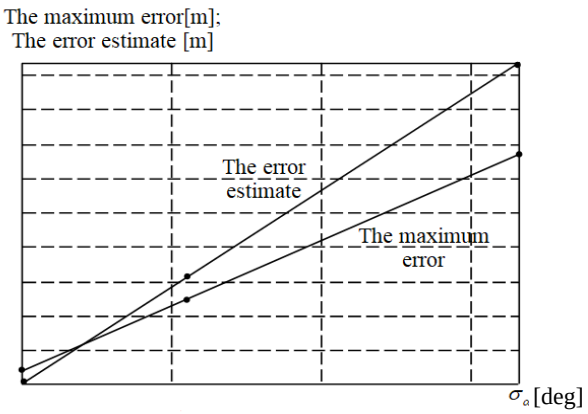

Fig. 5. The dependence of the maximum error, the error estimate on the MRC of the relief steepness.

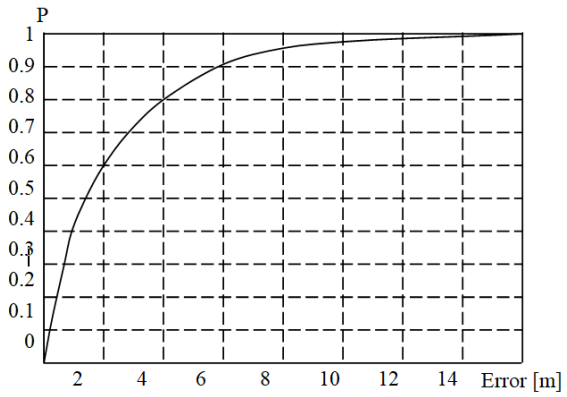

Fig. 6. Error probability graph.

In several tasks, constraints are imposed on the output parameters. Let us limit the maximum admissible error of the algorithm to 10 m. The results show that for DTM 1 and DTM 2, the maximum error lies within the specified tolerance, while for DTM 3, it does not. Let us determine the probability that the error for DTM 3 will not exceed the tolerance. For this, a program for constructing graphs of the dependence of the probability on the error has been developed. According to the graph (Fig. 6), the error will not exceed the tolerance with a probability of 97%. Similarly, it is possible to research other reliefs both in the absence and presence of the object composition.

VII. Conclusion

Researching the influence of the surface below on low-flying aircraft in practice requires many flights, which is very expensive and affects the pilot's psychology. Therefore, the proposed method allows the study of the influence of the underlying surface (terrain and object composition) on control algorithms for low-flying aircraft based on defining DTM and MRC libraries. DTM and MRC libraries are available to define various basic surfaces. It is proposed that flight reference paths on the DTM domain be enumerated during the simulation process to obtain statistical output information. Subsequent processing of the results compares the output information with the characteristics of the selected base surface to obtain analytical dependencies. The use of modern computing tools helps automate the proposed method, obtain convenient research tools, and increase the productivity of the technical workforce.

Conflict of Interest

The author declares no conflict of interest.

Acknowledgment

The author sincerely thanks the Air Defence-Air Force Academy, Ha Noi, Viet Nam.

References

[1] K. Andreev and E. Rubinovich, *UAV Guidance When Tracking a Ground Moving Target with Bearing-Only Measurements and Digital Elevation Map Support*, Southern Federal University, Engineering Sciences, Rostov Oblast, Russia, 2015. pp. 185–195.

[2] D. S. Sidorchuk and V. V. Volkov, "Fusion of radar, visible and thermal imagery with account for differences in brightness and chromaticity perception," *Sens. Syst.*, 2018, vol. 32, pp. 14–18.

[3] K. V. Andreev, "Optimal trajectories for unmanned aerial vehicle tracking the moving targets using linear antenna array," *Control Sci.*, 2015, vol. 5, pp. 76–84.

[4] B. M. Miller and E. Y. Rubinovich, "Impusive control in continuous and discrete-continuous systems," *IEEE Transactions on Automatic Control*, vol. 48, no. 12, 2003.

[5] K. S. Kolosov, "Robust complex processing of UAV navigation measurements," *Inf. Process*, vol. 17, pp. 245–257, 2017.

[6] R. C. Nelson, *Flight Stability and Automatic Control*, McGraw-Hill, 452, 1998.

[7] M. J. Fotuhi, Z. B. Hazem, and Z. Bingul, "Comparison of joint friction estimation models for laboratory 2 DOF double dual twin rotor Aero-dynamical system," in *Proc. 44th Annual Conference of the IEEE Industrial Electronics Society*, 2018, p. 6.

[8] Z. J. Xu *et al.*, "Digital mapping of surface turbulence status and aerodynamic stall on wings of a flying aircraft," *Nature Communications*, vol. 14, 2023.

[9] B. M. Miller, "Optimal control of observations in the filtering of diffusion processes I, II," *Autom. Remote Control.* vol. 46, pp. 207–214, 1985.

[10] B. M. Miller and W. J. Runggaldier, "Optimization of observations: A stochastic control approach," *SIAM J. Control Optim.*, vol. 35, pp. 1030–1052, 1995.

[11] C. Nicol, C. J. B. Macnab, and A. R. Serrano, "Robust adaptive control of a quadrotor helicopter," *Mechatronics*, vol. 21, no. 6, pp. 927–938, 2011.

[12] D. Abulkhanov, I. Konovalenko, D. Nikolaev, A. Savchik, E. Shvets, and D. Sidorchuk, "Neural network-based feature point descriptors for registration of Optical and SAR images," in *Proc. 10th International Conference on Machine Vision (ICMV 2017)*, 2017, pp. 13–15.

[13] S. Karpenko, I. Konovalenko, A. Miller, B. Miller, and D. Nikolaev, "Visual navigation of the UAVs on the basis of 3D natural landmarks," in *Proc. Eighth International Conference on Machine Vision ICMV 2015*, 2015, pp. 1–10.

[14] B. Miller, G. Miller, and K. Semenikhin, "Optimization of the data transmission flow from moving object to nonhomogeneous network of base stations," *IFAC Papers On Line*, vol. 50, pp. 6160–6165, 2017.

[15] J. Wijekoon, Y. Liyanage, and S. Welikala, "Yaw and pitch control of a twin rotor MIMO system," in *Proc. IEEE International Conference on Industrial and Information Systems (ICIIS)*, 2017, pp. 15–16.

[16] J. A. Vilchis, B. Brogliato, A. Dzul, and R. Lozano, "Nonlinear modelling and control of helicopters," *Automatica*, vol. 39, no. 9, pp. 1583–1596, 2003.

[17] C. Kanellakis and G. Nikolakopoulos, "Survey on computer vision for UAVs: Current developments and trends," *J. Intell. Robot. Syst.*, vol. 87, pp.141–168, 2017.

[18] I. Konovalenko, A. Miller, B. Miller, and D. Nikolaev, "UAV navigation on the basis of the feature points detection on underlying surface," in *Proc. 29th European Conference on Modelling and Simulation (ECMS 2015)*, 2015, pp. 499–505.

[19] A. Cesetti *et al.*, "Vision-based guidance system for UAV navigation and safe landing using natural landmarks," *J. Intell. Robot. Syst.*, vol. 57, pp. 233–257, 2015.

[20] B. M. Miller, G. B. Miller, and V. K. Semenikhin, "Optimal channel choice for lossy data flow transmission," *Autom. Remote Control*, vol. 79, pp. 66–77, 2018.

[21] K. S. Brentner and F. Farassat, "Modeling aerodynamically generated sound of helicopter rotors," *Progress in aerospace Sciences*, vol. 39, no. 2–3, pp. 83–120, 2003.

[22] M. Cakır, M. J. Fotuhi, and Z. B. Hazem, "Study of fuzzy control for pitch and yaw angles of two-degrees-of-freedom helicopter system," in *Proc. 2023 IEEE 8th International Conference on Engineering Technologies*, 2023, pp. 25–27.

[23] A. B. Miller and B. M. Miller, "Stochastic control of light UAV at landing with the aid of bearing-only observations," in *Proc. 8th International Conference on Machine Vision (ICMV)*, 2015, pp. 19–21.

[24] I. Konovalenko, A. Miller, B. Miller, A. Popov, and K. Stepanyan, "UAV control on the basis of 3D landmark bearing-only observations," *Sensors*, pp. 29802–29820, 2015.